Journal of Advanced Engineering Research
ISSN: 2393-8447
Volume 7, Issue 2, 2020, pp.69-77

Effect of Cavity Dimensions and Position in a Strut-Cavity Based Scramjet Combustor

Sumesh V[1,]*, Saran S Dharan[2]

[1,2]Department of Mechanical Engineering, College of Engineering Trivandrum, Kerala-695016, India

*Corresponding author email: sumeshcet@gmail.com

ABSTRACT

The aerothermodynamic processes in SCRAMJET propulsion system are complex and closely related. A significant challenge in these systems is to achieve an efficient air-fuel mixing and also to complete the combustion process within a very short residence time and finite combustor length. The combustion process cannot be initiated until mixing has been achieved at its stoichiometric level. In this study, a strut-cavity staged injection concept with a strut injector as the first stage and a cavity injector as the second stage injection is used. Cavity combustor can achieve flame-holding by the generation of subsonic recirculation region that ensures sufficient residence time. The dimensions of the cavity and its position in the mixing chamber are varied to obtain different configurations. These configurations are computationally investigated with both air and hydrogen as secondary injectant. Parameters such as momentum flux, degree of mixing, stagnation pressure loss and mixing efficiency are calculated for each configuration to analyse the extent of mixing. The position of the cavity inside the chamber is very important in determining the effectiveness of the mixing process. Cavities positioned at distance greater than x= 15 mm showed higher mixing rate than other positions. As the cavity length increases mixing efficiency also increases. Whereas, when the cavity depth increases the momentum flux distribution becomes more uniform indicating a uniform mixing. For a bigger cavity, higher mixing is achieved when positioned closer to the inlet of the mixing chamber. Whereas, smaller cavities can achieve faster mixing rate when positioned further downstream into the chamber. The mixing efficiency values are also in good agreement with the degree of momentum mixing values which indicate that for both hydrogen and air injection gives similar results regarding the cavity configurations.

Keywords – Cavity, Staged Injection, Strut, Supersonic Mixing.

1. INTRODUCTION

Hypersonic flows are generally defined as those flows with Mach number greater than 5. The most efficient regime of ramjet engine operation is around Mach 3 and its efficiency drops at hypersonic flow speeds. Supersonic Combustion RAMJET (SCRAMJET) is an improved version of ramjet engine which operates optimally at hypersonic speeds. The combustion process in a Scramjet engine is at supersonic speed. A stable, supersonic combustion process is necessary to ensure efficient engine operation at high flight mach numbers. A highly efficient mixing process is required to ensure efficient combustion. It is extremely challenging to attain effective mixing in a supersonic flow since the fluid residence time in the combustion chamber is very less of the order of 1-2 milliseconds. Increasing the mixing chamber length can enhance mixing but adds to the overall weight of the engine. So, with the constraint on the combustion chamber dimensions, effective mixing is to be achieved. The scramjet engine alters itself to various modes of operation throughout the entire flight. In cruise flight condition at high flight mach number, the scramjet mode of operation with a high-speed supersonic flow throughout the engine is essential. Whereas in climbing or descending stage at lower flight mach number, a ramjet mode of operation with subsonic combustor flow is required. For accommodating this wide spectrum of conditions, Dual-mode operation of a single engine is sought. They are termed as Dual Mode Ramjet Engines (DMRJ) [1].

The main airflow enters a Scramjet at hypersonic speed gets compressed by oblique shocks is mixed with the fuel in combustor and expands through nozzle to get the required thrust. For achieving high mixing effectiveness, different mixing augmentation techniques like active and passive methods can be employed. The active method comprises of inducing turbulence, shock interactions, swirls etc. into the flow by means of components like cavities, struts and so on. The passive method involves changing the inlet condition of the

flow by changing the geometry of the nozzle [2]. A strut is a geometrical structure which spans the entire width of the combustor. The strut offers fuel injection directly into the core of the mainstream and thus provides a rapid and uniform mixing. Masuya et al. [3] experimentally investigated the performance of a scramjet combustor using strut injectors and found out that mixing and combustion is more for large flow disturbing strut. Gerlinger and Bruggemann [4] numerically studied hydrogen injection through a strut in supersonic flow and the results showed that stagnation pressure loss strongly depends on trailing edge lip thickness. Length of the strut has only minor influence on stagnation pressure loss and mixing efficiency is independent of trailing edge lip thickness. When the fuel is injected parallel to the main flow the stagnation pressure losses are lessened which is higher in transverse and oblique injection methods. Sivasakthivel and Pandey [5] numerically studied mixing and combustion performance of a scramjet combustor with planar strut injector. The flame holding mechanism of a planar strut was analysed computationally with both cold flow and engine ignition. The eddies generated in the strut behaves like a flame holder in the combustion chamber and prolong the residence time. The stream-wise vortices generated improves the air-fuel mixing process. Recirculation regions are formed at the trailing edge of the strut which behaves like a flame holder for combustion process [6].

Cavity based mixing augmentation technique uses a backwards-facing step geometry on the wall surface is to induce re-circulation and have better flame holding capability. There are two counter-rotating lobes formed inside the cavity, one bigger primary lobe and other a smaller secondary lobe. Ken et al. [7] experimentally studied the flame holding and mixing characteristics of supersonic reacting flow over acoustically open cavities. The results indicated that cavities with a short aspect ratio provided good flame holding, and those with a relatively long aspect ratio shortened the flame length substantially via acoustic excitation. To eliminate the generation of travelling shocks within the cavity and also to suppress the unsteady nature of the free shear layer, a cavity with an inclined aft wall at the trailing edge can be employed [8], [9]. Gruber et al. [10] investigated both experimentally and numerically the flow field associated with several cavity-based flame holders in a non-reacting supersonic flow. Analysis indicated that the ramp angle plays a prominent role in determining the character of the shear layer that spans the cavity. Decreasing the aft wall angle will promote a more acoustically stable cavity flow and improved entrainment because the shear layer impinges deeper into the cavity. Reducing the ramp angle decreases the size of the secondary lobe. They also inferred that the cavity length determines mass entrainment whereas the cavity depth determines residence time. During the combustion process, the pressure rise in the combustor may propagate up-stream along the boundary layer causing flow-separation and penetrates inlet section resulting in an un-started condition of the engine called combustor–inlet interaction [11]. With the limitation of peak pressure at the minimum cross-sectional area, to maximize the thrust and also to avoid combustor–inlet interaction, an additional pressure rise in downstream section of the combustor becomes essential. Thus, a staged injection concept is employed. The staged injection also increases the overall equivalence ratio and also reduces the risk of thermal choking in the combustor [12]. A staged injection uses multiple stages of same or different injection techniques and combines the advantages of the injection methods used. The strut injector supply fuel to center portion of the primary air-stream, thus the spread of fuel stream will be limited to the core section. There will be oxidiser concentration remaining in the sides of the combustor walls which can be utilised to get more thrust. The Wall based injectors supply fuel to the sides of combustor walls. Since the penetration power of such injection methods is less, they remain in the outer region of the combustor and may not reach the core region of the flow. A combination of these methods can provide effective utilization of oxidiser and fuel.

The current investigation computationally studies the effects of the position of the cavity and its dimensions in accelerating the mixing process in a strut-cavity based scramjet combustor. Multistage injection with strut-based injection method as the first stage and a cavity injection method as the second stage is employed. Different cavity configurations are investigated and compared based on some performance parameters with both hydrogen and air as secondary injection.

2. METHODOLOGY

2.1 Geometry Details

The main components of the experimental setup are a settling chamber, nozzle and a mixing chamber. The primary air is supplied to the inlet of the settling chamber which is 100 mm in length with a cross-sectional area of 24 × 28 mm^2. The air then passes on to

the nozzle where the flow is accelerated and then into the mixing chamber of length 150 mm. A planar strut injector of length 91 mm, trailing edge height 6 mm and half-angle 26.56° is taken for the first stage injection. The fuel injection is given through 2 mm ports provided along the trailing-edge of the strut injector. The strut is placed inside the nozzle in such a way that the minimum area is attained at the nozzle throat. This gives a new area ratio of 2.25, which yields a Mach no. of 2.32 at the nozzle exit. The strut injector is followed by an inclined aft wall cavity which is used as the second stage injection method.

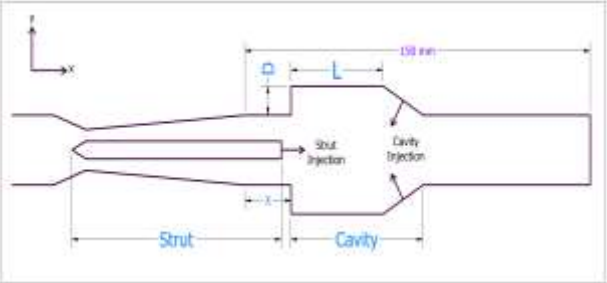

Fig. 1. Strut-cavity assembly

The cavity can be positioned at various locations within the mixing chamber. The strut-cavity assembly is depicted in Fig. 1. Here, "x" is the cavity position in the mixing chamber from the chamber inlet, "L" denotes the length of the cavity, "D" is the cavity depth. The ramp angle is taken as 30°. Injection is given from 2 mm ports at the middle of the ramp and normal to it. Air is initially used as the secondary injectant and then hydrogen fuel is used for each configuration. Different configurations are to be analysed based on the performance parameters for an optimum configuration.

2.2 Computational Details

The analysis is done using Ansys Fluent. The pressure based (coupled) double precision solver with least squares cell based spatial discretization and second order upwind interpolation scheme is used on a 2-D planar geometry.

2.2.1 Governing Equations: The steady, 2-D, Reynolds-Averaged Navier-Stokes (RANS) equation is solved along with the Shear Stress Transport (SST), k-ω turbulence model and ideal gas equation of state. The three-coefficient viscosity Sutherland's law was defined for viscosity. The basic governing equations are:

Continuity Equation:

$$\nabla \cdot (\rho \vec{v}) = 0 \quad (1)$$

Momentum Equation:

$$\nabla \cdot (\rho \vec{v}\vec{v}) = -\nabla P + \nabla \cdot \mu \left[(\nabla \vec{v}) - \frac{2}{3} \nabla \cdot \vec{v} I \right] \quad (2)$$

Energy Equation:

$$\nabla \cdot \vec{v}(\rho E + P) = \nabla \cdot \left[\left(k_T + \frac{c_p \mu_t}{\mathrm{Pr}_t} \right) \nabla T + \mu_{\mathrm{eff}} \left[(\nabla \cdot \vec{v}) - \frac{2}{3} \nabla \cdot \vec{v} I \right] \cdot \vec{v} \right] \quad (3)$$

In the above equations, P denotes static pressure, ρ denotes the density, μ denotes the molecular viscosity, Pr denotes the Prandtl number, I denote the unit tensor, T denotes the temperature, E denotes the total energy, and k_T denotes the thermal conductivity.

2.2.2 Boundary Conditions: An extended domain of length 750 mm and height 300 mm is taken for analysis as shown in Fig. 2. The main airflow to the settling chamber is supplied at a total pressure of 1 MPa. Secondary inlets are defined at a stagnation pressure of 0.2 MPa at strut trailing edge and cavity inlets. The turbulent intensity at the inlet is considered as 5% whereas the value of hydraulic diameter for the primary inlet and secondary inlet is 25.846 mm and 2 mm, respectively. The outlet condition is defined as atmospheric pressure and temperature. No-slip boundary condition is assumed to all the solid surfaces (walls and strut geometry).

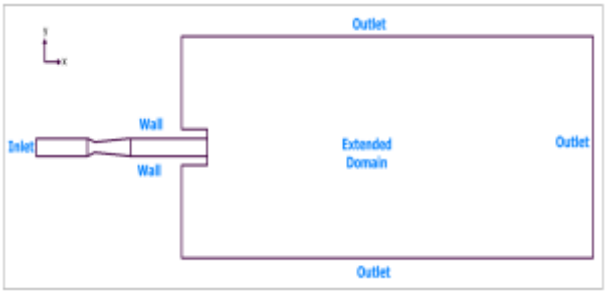

Fig. 2. Computational Domain

2.2.3 Grid Independence Study: From the parametric analysis for determining the minimum mesh element size for grid convergence three mesh structures are chosen, a coarse mesh with 76648 elements, a medium mesh with 163196 elements and a fine mesh with 290911 elements. No appreciable variation in the static pressure values with different grid sizes are observed from the static pressure distribution along the length for the above grids shown in Fig. 3, indicates grid convergence.

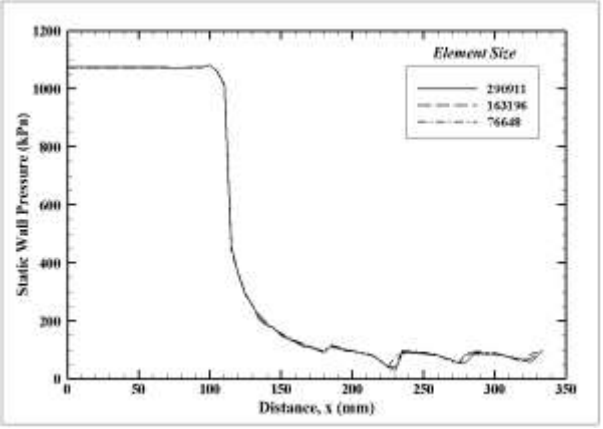

Fig. 3. Static wall pressure distribution

2.3 Performance Parameters

2.3.1 Momentum Flux Distribution (MFD): The primary and secondary streams enter the chamber at different momentum and stagnation pressures. The uniformity of the distributions of momentum flux and stagnation pressure at the exit plane of the mixing chamber is considered as the measure of the extent of bulk mixing [13]. The Momentum Flux (ψ) is given as:-

$$\psi = P\left(1+\gamma M^2\right) \tag{4}$$

Here, P denotes the static pressure at exit plane, M denotes the mach number at exit plane and γ denotes the specific heat ratio.

2.3.2 Degree of Momentum Mixing (DOM): For quantitatively assessing the mixing performance of different configurations, a mixing parameter called the Degree of Momentum Mixing (DOM) [13] is used which is given by:-

$$\mathrm{DOM} = \frac{(\phi - \phi_{\mathrm{um}})}{(1-\phi_{\mathrm{um}})} \tag{5}$$

Where, φ is the uniformity factor expressed as:-

$$\phi = 1 - \frac{\sigma}{\mu} \tag{6}$$

here, σ denotes the standard deviation of momentum flux along the chamber exit plane, μ denotes the average value momentum flux at chamber exit plane, φ_{um} denotes the uniformity factor for unmixed condition ie., when the two streams are totally unmixed. Degree of momentum mixing will be equal to unity when the two streams are fully mixed and will be equal to zero when two streams are completely unmixed. DOM represents the extent of mixing achieved.

2.3.3 Stagnation Pressure Loss (SPL): As far as Scramjet combustors are concerned minimizing the stagnation pressure loss is an important criterion for maximizing thrust generation. The stagnation pressure loss across the mixing chamber is evaluated by taking the area weighted average of stagnation pressure at inlet and exit plane of the chamber. The Percentage Loss in Stagnation Pressure (SPL) is calculated as:-

$$\mathrm{SPL} = 1 - \frac{\Sigma}{\Sigma}\frac{P_o A_o}{P_i A_i} \tag{7}$$

2.3.4 Mixing Efficiency: Mixing efficiency is the fraction of least available reactant that can react as the mixture is brought to chemical equilibrium [14]. The mixing efficiency (η_m) at any particular axial location is defined as:-

$$\eta_{m(x)} = \frac{\int \alpha_R \rho u dA}{\int \alpha \rho u dA} \tag{8}$$

where, ρ denotes the density and u denotes the velocity of hydrogen at a given section. A is the cross-sectional area of the axial station where mixing is evaluated. α_R= Mass fraction of the least available reactant that would react if complete reaction took place without further mixing and is given by,

$$\alpha_R = \left\{ \begin{array}{ll} \alpha, & \alpha \le \alpha_s \\ \alpha_s\left(\frac{1-\alpha}{1-\alpha_s}\right), & \alpha > \alpha_s \end{array} \right\} \tag{9}$$

In the above equations, α denotes fuel mass fraction at the axial location under evaluation and α_s is the injectant stoichiometric mass fraction. For Hydrogen, α_s= 0.0285. The value of mixing efficiency changes from 0 to 1. η_m= 0 represents a state where the two streams are unmixed and η_m= 1 indicates a perfectly mixed system. The plane where η_m reaches unity gives the Mixing Length L_{mix} at which all the fuel gets mixed with the main stream.

2.4 Validation of Numerical Solver

The numerical solver is validated and its correctness is ascertained by comparing computational and experimental data of a planar strut injector. The experimental investigation on the baseline case of a planar strut placed inside a mixing chamber of length 150 mm without a cavity is done and is cross-referenced with computational value to determine the correctness of the solver. The comparison of DOM values is given below in Table 1. The value of Degree of Momentum Mixing for both the experimental and

numerical investigations are both comparable and a difference of 2% is within an acceptable range.

Table 1. Comparison of available experimental and numerical data

	DOM(%)
Experimental	28
Numerical	30.17

3. RESULTS AND DISCUSSIONS

The length, depth and position of the cavity in the mixing chamber are varied to different dimensions. Cavity depth values of 5 mm, 10 mm and 15 mm are taken. For each cavity depth corresponding cavity lengths with L/D ratio of 2, 3, 4, 5 and 6 are taken. The position of the cavity in the mixing chamber is taken as 0, 5, 10, 15, 20 and 25 mm from the inlet of the mixing chamber for different configurations.

3.1 Cavity Length variation with a fixed Depth of 5 mm

For the cavity depth of 5 mm, L/D ratio and positions of the cavity are varied to different dimensions. Each configuration is analysed first with air injection and then with hydrogen injection. The DOM values are calculated and graphically summarized in Fig. 4

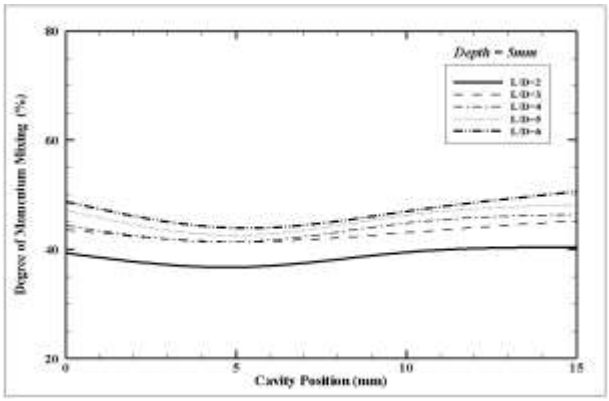

Fig. 4. DOM for different configurations with cavity depth of 5 mm

The SPL values are calculated and graphically summarized in Fig. 5.

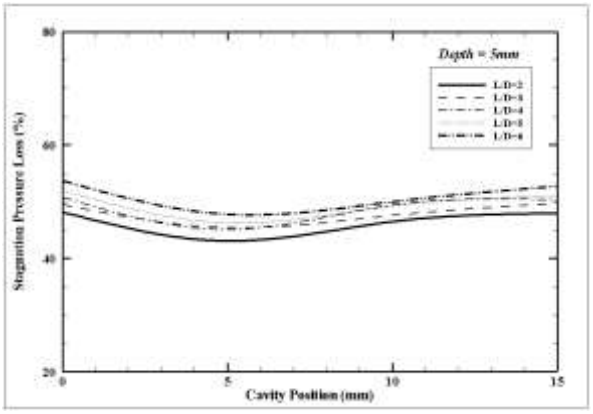

Fig. 5. SPL for different configurations with cavity depth of 5 mm

Higher DOM and SPL values are obtained for the cavity placed at the inlet of the mixing chamber and a distance greater than 15 mm inside the chamber. It is also seen that for higher cavity L/D ratio higher DOM values are obtained.

The MFD at the exit plane for different cavity configurations with depth 5 mm is shown in Fig. 6.

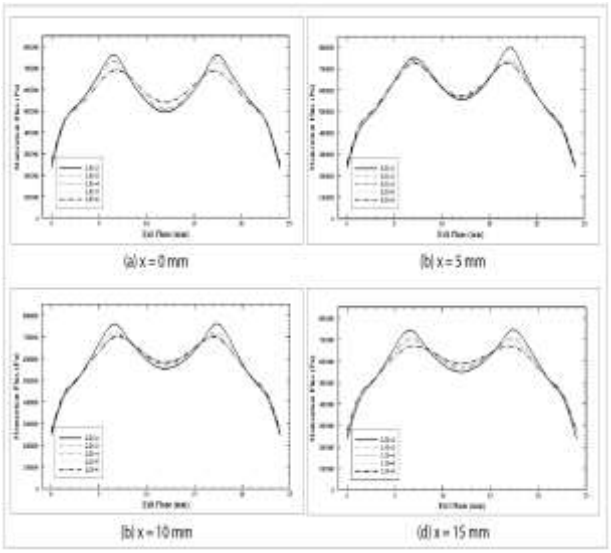

Fig. 6. MFD for a cavity depth of 5 mm at different positions

The MFD becomes more uniform as cavity L/D increases. The cavity positions at 0 mm and 15 mm provided more uniform mixing than other positions. All the configurations are analysed with hydrogen injection and the mixing efficiency values are calculated and graphically summarized in Fig. 7.

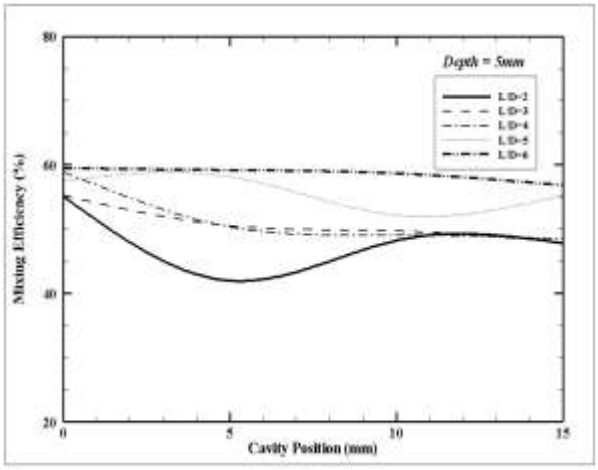

Fig. 7. Mixing efficiency for a cavity depth of 5 mm at different positions

The mixing efficiency values are comparable with the DOM values. When the L/D ratio increases, higher mixing efficiency is achieved. The cavity position x= 0 mm, yields higher efficiency than other nearby positions. Since the depth of the cavity is small higher L/D ratios may be required for attaining better mixing. So, a cavity with larger depth is analysed.

3.2 Cavity Length variation with a fixed Depth of 10 mm

For analysing the effect of depth of the cavity, the cavity depth is increased to 10 mm. Various L/D ratios and cavity positions are analysed with air injection and hydrogen injection. The DOM and SPL values are calculated and graphically summarised in Fig. 8 and Fig. 9 respectively.

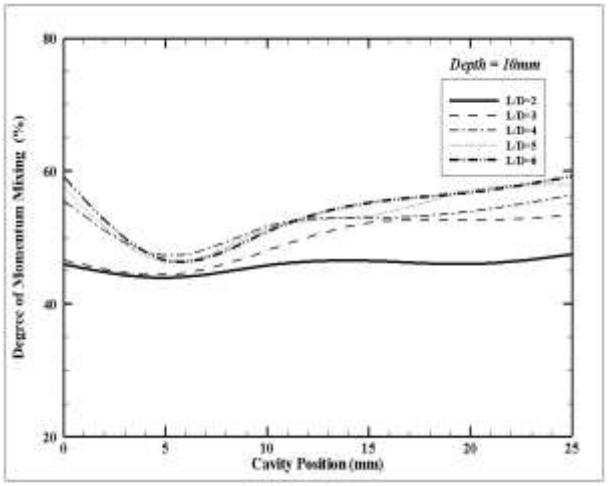

Fig. 8. DOM for different configurations with cavity depth of 10 mm

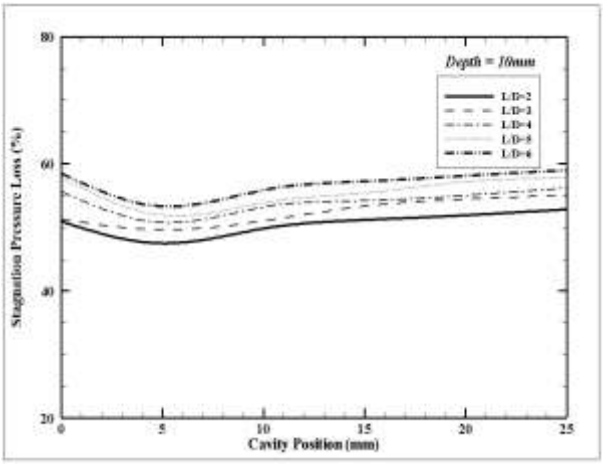

Fig. 9. SPL for different configurations with cavity depth of 10 mm

The trend of DOM and SPL values of 10 mm depth is similar to the earlier results for 5 mm depth. Higher DOM and SPL values are obtained for the cavity positioned at 0 mm and 15 mm inside the chamber. It is also seen that for higher cavity L/D ratio higher DOM values are obtained. The MFD at the exit plane for different cavity configurations with depth 10 mm is shown in Fig. 10.

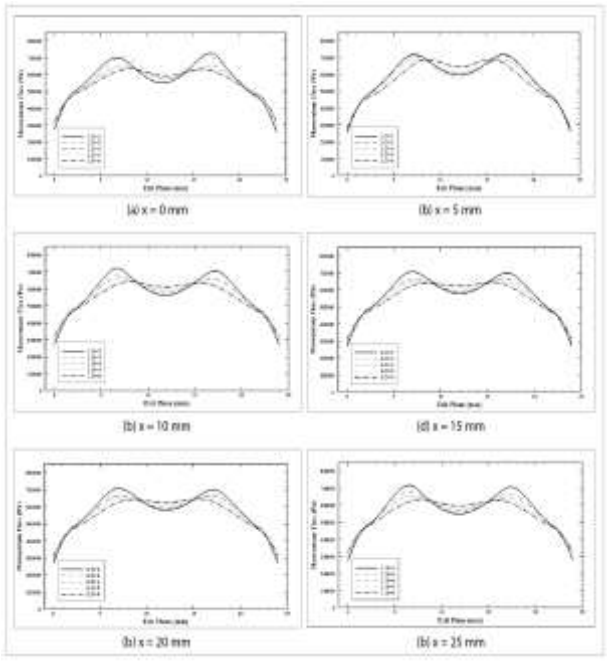

Fig. 10. MFD for a cavity depth of 10 mm at different positions

The MFD infers that as the cavity L/D ratio increases the mixing becomes more uniform. An L/D of 6 is enough to achieve a uniform momentum flux distribution and hence uniform mixing.

All the configurations are further analysed with hydrogen injection and the mixing efficiency values are graphically summarized in Fig. 11.

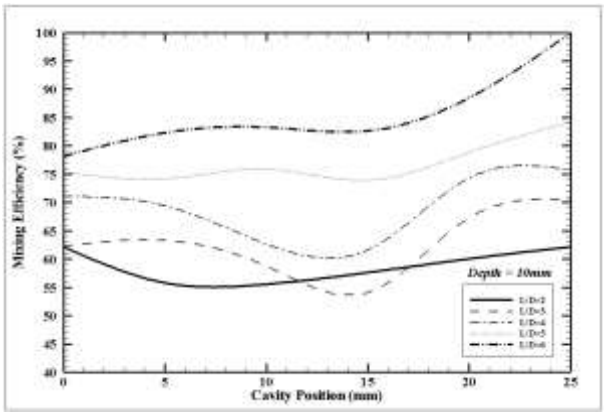

Fig. 11. Mixing efficiency for a cavity depth of 10 mm at different positions

The mixing efficiency values points out some important results. For the cavity positioned at a distance of 25 mm, maximum efficiency is attained at an L/D ratio of 6. It means that the mixing length for a cavity of L/D= 6 is less when the cavity is placed downstream into the mixing chamber. Bigger cavities can attain higher mixing rates when positioned closer to the chamber inlet. As the mixing chamber length is limited to know the effects of a bigger cavity the cavity depth can be further increased.

3.3 Cavity Length variation with a fixed Depth of 15 mm

For the cavity depth of 15 mm different L/D ratios and positions are analysed with air and hydrogen injection. The DOM values are calculated and graphically summarized in Fig. 12.

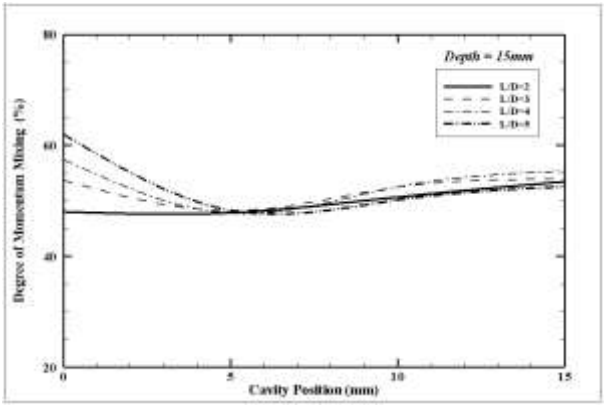

Fig. 12. DOM for different configurations with cavity depth of 15 mm

The SPL values are calculated and graphically summarized in Fig. 13.

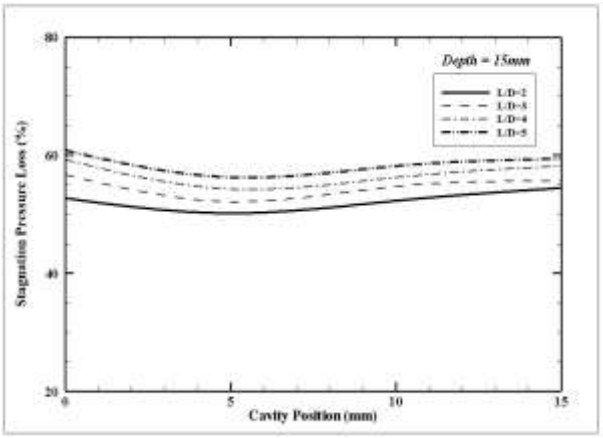

Fig. 13. SPL for different configurations with cavity depth of 15 mm

The DOM and SPL values show the same trend as observed for 5 mm and 10 mm depths. As the cavity L/D ratio increases, the DOM value also increases.

The MFD at the exit plane for different cavity configurations at each cavity position is plotted shown in Fig. 14.

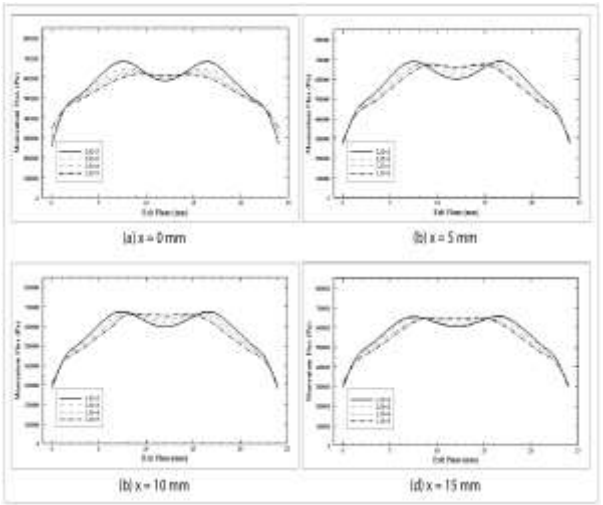

Fig. 14. MFD for a cavity depth of 15 mm at different positions

The MFD is uniform for all the configurations except L/D= 2. The MFD is more uniform for cavities with a higher L/D ratio. This uniformity is due to the greater depth of the cavity compared to the previous results. All the configurations are further analysed with hydrogen injection and the mixing efficiency values are graphically summarized in Fig. 15.

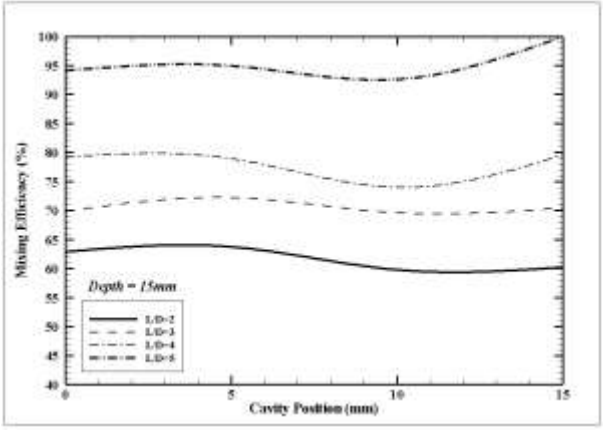

Fig. 15. Mixing efficiency for a cavity depth of 15 mm at different positions

The mixing efficiency values support the results obtained in earlier studies. The cavity with an L/D of 5 achieves 100% efficiency at a distance of 15 mm into the chamber. Smaller cavities can achieve faster mixing rate when positioned further downstream into the chamber. Larger cavities cannot be used because larger cavities can make the engine bulkier and will produce more drag which is not desirable.

4. CONCLUSION

The degree of mixing, percentage loss in stagnation pressure, momentum flux distribution and mixing efficiency are calculated for different configurations. The position of the cavity inside the chamber is very important in determining the effectiveness of the mixing process. Cavities positioned at distance greater than x= 15 mm showed higher mixing rate than other positions. Cavities positioned at x= 0 mm gave higher mixing rate than at other nearby positions like 5 mm and 10 mm. As the cavity length increases mixing efficiency also increases along with the stagnation pressure loss. As the cavity depth increases the momentum flux distribution becomes more uniform indicating a uniform mixing. For a bigger cavity, higher mixing is achieved when positioned closer to the inlet of the mixing chamber. Whereas, smaller cavities can achieve faster mixing rate when positioned further downstream into the chamber. As the degree of mixing increases, the stagnation pressure loss also increases, which means that better mixing is achieved at the expense of stagnation pressure loss. The mixing efficiency values are also in good agreement with the degree of momentum mixing values which indicate that for both hydrogen and air injection gives similar results regarding the cavity configurations.

NOMENCLATURE

P	Static Pressure
P_o	Stagnation Pressure
M	Mach Number
A_e	Exit Area of the Nozzle
A_t	Nozzle Throat Area
x	Position of the Cavity in the Chamber
u	Velocity
D	Depth of the Cavity
L	Length of the Cavity
θ	Aft-Ramp Angle of the Cavity
ρ	Density
γ	Specific Heat Ratio
φ	Uniformity Factor
ψ	Momentum Flux
σ	Standard Deviation of Momentum Flux
μ	Average Value Momentum Flux
η_m	Mixing Efficiency
α	Fuel Mass Fraction
α_s	Injectant Stoichiometric Mass Fraction
α_R	Reactant Mass Fraction

REFERENCES

[1] T V Venkateswaran, “Scramjet: Isro’s futuristic technology to reduce costs of space travel” *i Wonder,* (3), 2017, 310–324.

[2] Tan Jianguo, Zhang Dongdong and Lv Liang, “A review on enhanced mixing methods in supersonic mixing layer flows” *Acta Astronautica,* 152, 2018, 310–324.

[3] Goro Masuya, Tomoyuki Komuro, Atsuo Murakami, Noboru Shinozaki, Akihiro Nakamura, Motohide Murayamall and Katsura Ohwaki, “Ignition and combustion performance of scramjet combustors with fuel injection struts” *Journal of Propulsion and Power,* 11, 1995, 301–307.

[4] P Gerlinger and D Bruggemann, “Numerical investigation of hydrogen strut injections into supersonic airflows” *Journal of Propulsion and Power,* 16, 2000, 22–28.

[5] KM Pandey and T Sivasakthivel, “CFD analysis of mixing and combustion of a scramjet combustor with a planer strut injector” *International Journal of Environmental Science and Development,* 2, 2011, 102.

[6] Juntao Chang, Junlong Zhang, Wen Bao and Daren Yu, “Research progress on strut-equipped supersonic combustors for scramjet application”

Progress in Aerospace Sciences, 103, 2018, 1–30.

[7] Ken H Yu, Ken J Wilson and Klaus C Schadow, "Effect of flame-holding cavities on supersonic-combustion performance" *Journal of Propulsion and Power*, 17, 2001, 1287–1295.

[8] Kyung Moo Kim, Seung Wook Baek and Cho Young Han, "Numerical study on supersonic combustion with cavity-based fuel injection" *International Journal of Heat and Mass Transfer*, 47, 2004, 271–286.

[9] William Allen, Paul King, Mark Gruber, Campbell Carter and Kuang-Yu Hsu, "Fuel-air injection effects on combustion in cavity-based flameholders in a supersonic flow" *41st AIAA/ASME/SAE/ASEE Joint Propulsion Conference & Exhibit*, 2005, 4105.

[10] M R Gruber, RA Baurle, T Mathur and K-Y Hsu, "Fundamental studies of cavity-based flameholder concepts for supersonic combustors" *Journal of Propulsion and power*, 17, 2001, 146–153.

[11] Sadatake Tomioka, Atsuo Murakami, Kenji Kudo and Tohru Mitani, "Combustion tests of a staged supersonic combustor with a strut" *Journal of Propulsion and power*, 17,2001, 293–300.

[12] Sirka Fuhrmann, Andreas Hupfer and Hans-Peter Kau, "Investigations on multi-stage supersonic combustion in a model combustor" *17th AIAA International Space Planes and Hypersonic Systems and Technologies Conference*, 2011, 2332.

[13] BVN Charyulu, J Kurian, P Venugopalan and V Sriramulu, "Experimental study on mixing enhancement in two dimensional supersonic flow" *Journal of Propulsion and power*, 24, 1998, 340–346.

[14] Marlon Mao, David W Riggins and Charles R Mcclinton, "Numerical simulation of transverse fuel injection", *In NASA, Lewis Research Center, Computational Fluid Dynamics Symposium on Aeropropulsion*, 1991, 635-667.